Mathematical Analysis and Design of a Novel 5-DOF 3D Printer Robotic System

Ahmet Dumlu[1, *], Mehran Mahboubkhah[2], Kagan Koray Ayten[1], Gurkan Kalinay[1]
[1]*Department of Electrical & Electronics Engineering, Erzurum Technical University, Erzurum, Turkey*
[2]*Faculty of Mechanical Engineering, Tabriz University, Tabriz, Iran*
ahmetdumlu@erzurum.edu.tr

***Abstract*—In this study, the mathematical analysis and design of a new 3D printer with 5 degrees of freedom were carried out. Thanks to the developed system, a new concept has been brought to the multi-axis 3D printer mechanisms, and thus, it is aimed to improve the part quality in additive manufacturing (AM) processes. As a result of adding the 4th and 5th axes to the moving platform of the system, the production time of the part was accelerated. It is also possible to print more complex and curved shapes with less support. To design a system with these features, first of all, the kinematic analysis of the system was obtained using vector algebra, and the workspace of the current printer was determined by considering the system constraints in this article. By giving detailed information about the mechanical and electrical components of the designed system, the working principle of the whole system is presented. According to the findings obtained in the studies, the kinematic analyses performed for the proposed system proved to be correct and a new system was proposed especially for additive manufacturing technologies.**

***Index Terms*—Additive manufacturing; Parallel manipulator; Kinematics; Workspace.**

I. INTRODUCTION

Additive manufacturing technology is seen as an important part of the third industrial revolution. It has also revolutionized the manufacturing industry and attracted intense interest in the literature [1], [2]. In particular, since products with complex geometries can be produced by additive manufacturing technology, there are many studies in the literature to further improve this technology. Generally, these studies aim to increase the strength and wavy surface quality of the product to be produced, as well as to shorten the production time. However, in traditional 3-degree-of-freedom (DOF) linear machine tools or printers, parts called "supports" are used to produce the workpiece, and therefore the use of these parts increases the production cost. To avoid the disadvantages listed above, systems with higher degrees of freedom or different kinematic structures have been designed instead of the classical 3-axis systems used in additive manufacturing technologies in recent years. In particular, it has been stated that if multi-axis robotic systems with parallel kinematics are used in additive manufacturing technologies, it allows the production of parts with complex geometries and restrictions can easily be avoided [3].

Mechanisms with a parallel kinematic structure have been preferred in many production studies, especially for additive manufacturing technologies, since they have higher accuracy and processing speed compared to cartesian systems. In the literature, a rotational motion has been added to the z-axis to shorten the production time in different parallel kinematic systems.

In [4], the authors developed a parallel hybrid mechanism with 5 degrees of freedom for industrial Computer Numerical Control (CNC) application. All kinematic and mathematical analyses of this system developed in their study were presented in detail. As a result of the dynamic analysis, the position and force switching control method has been developed. To evaluate the performance of hybrid machines consisting of a parallel kinematic structure, the authors conducted a series of experiments, including circular contouring experiments, positioning accuracy, and shear testing. Clavel [5] describes the new invention of a parallel Delta robot with three or more parallel kinematic chains (axes) to solve all the problems and limitations. In [6], a high-speed parallel robot with Schönflies motion was introduced. This robot showed promising prospects for performing high-speed pick-and-place manipulation for packaging production lines. A line graph method based on Grassmann line geometry was used to investigate the mobility characteristics of the proposed robot. Then, inverse kinematics is derived, and the singularity of the robot is investigated using both qualitative and quantitative approaches. In [7], a new family of fully parallel robots is presented that provides 3 translations and 1 rotation about a given axis. Such machines are intended for use in robotic or machining. The ability of the proposed structure to provide the required DOF was first demonstrated. The position and velocity relations are given. Finally, constructive designs are presented that demonstrate the effectiveness of the solution with linear or rotary actuators. In [8], a new 4-DOF parallel mechanism was presented to handle heavy parts in a large work area. These 4 degrees of freedom are 3 translations and 1 rotation about a given axis. Such a mechanism is rare; most common parallel mechanisms have 3 or 6 degrees of

Manuscript received 28 February, 2022; accepted 28 May, 2022.
This research was supported by the TUBITAK under Grant No. 119N707.

freedom. In [9], the main purpose of this article is the kinematic optimization of a 5-DOF parallel kinematic mechanism (PKM) robot for additive manufacturing. The kinematics of the robot is examined and a genetic algorithm is used to optimize the machine parameters to cover a specific work area, as well as the design and control system of the robot. In [10], the article is about the conceptual design and dimensional synthesis of a parallel linear Delta robot for additive manufacturing. In conceptual development, the quality function deployment (QFD) matrix is used to transform user requirements into design parameters. In [11], the design and implementation of a prototype of a delta parallel robot-based 3D printer were described. This robot reduced the printing time without sacrificing the quality of the final product. For the height calibration of the printer dock, an automatic levelling system has been developed employing an inductive sensor to avoid manual use. In [12], the development of a new Coordinate Metrology Machine (CMM) with a new 4-DOF parallel kinematics, namely C4, three translations, and one rotation about the x-axis, was presented. After a systematic design refinement process, the various design parameters and details of the components were analyzed to select the optimum mechanism with the greatest dexterity and rigidity without single spots in a well-formed workspace. The final design was validated by building a fully functioning prototype of the mechanism and experimentally testing several case studies. Thus, these systems were raised to 4 degrees of freedom [4]–[12]. In another study, a system with a delta-type parallel kinematic structure was provided with the ability to rotate to the x-axis, thus increasing the mobility of the system [12].

In this study, unlike the studies and literature mentioned above, a concept design of a new 3D printer capable of rotation in the x-axis and z-axis with 5 degrees of freedom has been made and implemented differently from [9]. In [9], the translational motion is performed by a Delta robot with 3 degrees of freedom, while the rotational motion is performed by 2 separate independent motors placed on the moving table. These rotational motions are carried out with the help of motors, independent of the kinematic analysis of the 3D printer.

In the proposed study, 3 translational and 1 rotational motion can be provided with the help of legs connected to 4 separate motors used in the system. The fifth degree of freedom is provided with the help of a separate motor placed on the table. Therefore, the rotation motion in the x-axis, which is necessary for fast part production, is realized by the interdependent kinematic analysis of the system. Due to this feature, unlike the system given in [9], our kinematic structure works simultaneously as a whole, and as a result, more precise and faster part production is achieved. In addition to the above, thanks to the rotational motion of the proposed system to the x-axis and z-axis, it is aimed to create curved layers parallel to the part surface, and in this way, it is aimed to avoid the need for support parts in the production process, unlike classical systems. To achieve these goals, first, the kinematic analysis of the proposed system is presented in detail using vector algebra. The system workspace was determined by simulations made in the CATIA software. The accuracy of the kinematic analyses made for the system has been proven in the tests performed using CATIA software. In addition, to determine the Jacobian matrix of the system, information about velocity kinematic analysis is also presented in this study.

In this study, both the mechanical and electrical components of the system were introduced, and the concept design of the entire system was presented in detail. The main contribution of this study to the literature is to provide information about the concept design of a new parallel kinematic structure 3D printer, which can reduce production costs and operate more sensitively at higher speeds, unlike conventional 3D printers. According to the experimental results obtained, the mathematical analyses for this new system have been proven to be correct.

II. CONCEPT DESIGN OF 5-AXIS 3D PRINTER

The designed 3D printer system consists of a fixed and mobile platform connected by four kinematic chains in total (two PR(Pa)R and two PR(Pa)U), as shown in Figs. 1(a) and 1(b). Figure 1(a) shows the structure of the proposed 5-DOF parallel mechanism. Figure 1(b) shows links and mobile platforms of 5 proposed DOF Parallel Mechanism in its structure.

Here, P, R, Pa, and U represent prismatic, rotary, parallelogram, and universal joints, respectively. The main component of these kinematic chains is the planar four-bar parallelogram structure. These structures are manipulated by employing four cars mounted on an independent linear rail system. To create the parallelogram structure, each of the cars on the system is connected to each link separately with the help of spherical joints. At the other end, the joints for the second and third arms are connected to the moving platform via ball joints, and the joints for the first and fourth arms are indirectly connected to the moving platform. Each connector is connected to the moving platform by a swivel joint. For the present manipulator, the floating platform has 3-DOF translational and 1-DOF rotational mobility in the x-direction (see Figs. 1(a) and 1(b)). As seen in Fig. 1(a), 5 different stepper motors are used in the system. The task of the 4 motors in the base part of the system is to give the system 3 translational movements and a rotational movement in the x-direction. These movements can be realized with the kinematic analysis described in Section III. The 5th stepper motor, which is mounted on the moving platform of the system, gives the system independent rotational motion in the z-direction. This movement is independent of kinematics, and rotation of the part to be produced is provided with a separate command. In other words, the rotational mobility required for the z-direction is provided by a turntable.

The configuration of the components of the parallel mechanism designed and modelled using CATIA software is demonstrated in Fig. 2. In addition, numbered stepper motors placed at the bottom of the system are shown in Fig. 2. These motors provide 3 translational and 1 rotational motion of the moving table according to the kinematic equations of the system. If the moving table is desired to move only in the z-direction, these 4 motors must rotate at equal rotational amounts, and thus move the saddles up or down at the same distance. In addition, if the moving table needs to make translational movement only in the x-axis at a

certain z height, then only the 3rd motor needs to rotate at a certain step according to the kinematic analysis. Similarly, if it only needs to make translational movement in the y-axis, then only the 2nd motor needs to rotate at a certain step. Finally, if the moving table needs to rotate around the x-axis, only the 1st and 3rd motors need to rotate in a certain step in the opposite direction relative to each other.

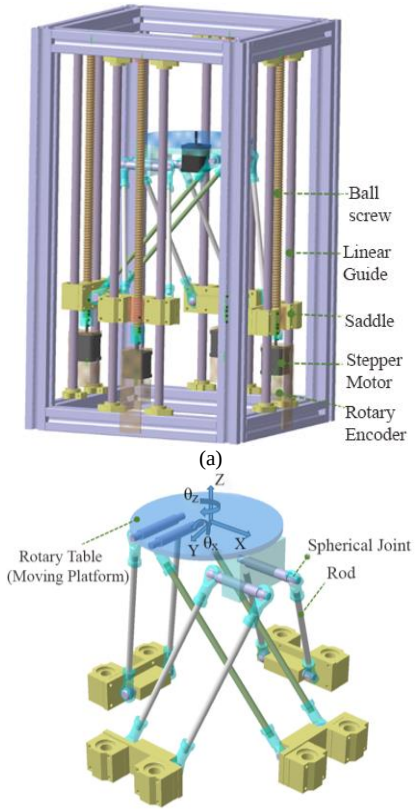

Fig. 1. (a) Structure of the proposed 5-DOF parallel mechanism; (b) Links and mobile platform of the 5-DOF parallel mechanism proposed.

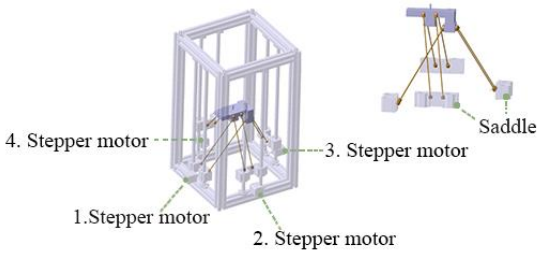

Fig. 2. Configuration of the 5-DOF 3D printer.

III. MATHEMATICAL MODELLING OF THE RECOMMENDED 5-DOF 3D PRINTER

In this section, detailed information on the kinematics and workspace analyses for the system is presented. First, considering the rigid body modelling of the proposed system, inverse kinematic analysis was performed with the vector approach. Then, the workspace analysis of the mechanism was carried out considering the obtained kinematic equations and the constraints of the system. Finally, studies on the kinematic analysis of the velocity and acceleration of the mechanism were carried out.

A. Inverse Kinematics of the Recommended 5-DOF 3D Printer

When we give the position and orientation values of the mobile platform, the inverse kinematic analysis calculates the angular positions of the joints that will bring the mobile platform to these position and orientation values. To be able to control the system correctly and at the same time reveal the dynamic model of the system, this kinematic analysis must be presented correctly. Especially the J codes that need to be determined during the manufacturing of a part are obtained with the help of this kinematic analysis. The position that the movable table should reach during the manufacture of any part is converted into leg lengths thanks to the given kinematic equation. These leg lengths are given by the linear guide. In one complete revolution of the motor, the linear guide moves proportionally. In the literature, different methods are used for the kinematic analysis of different types of parallel mechanisms. These are the Denavit-Hartenberg method, vector algebra method, geometric approach, and Bezout methods. In addition, genetic and Nelder-Mead algorithms have been used for kinematic analysis in recent years.

In this study, the vector algebra method was used for the inverse kinematic analysis of the mechanism. To perform the analysis, a vector diagram of the system is shown in Fig. 3.

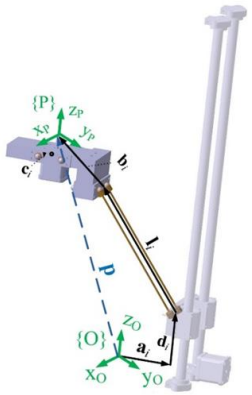

Fig. 3. Vector notation for kinematic modelling of the system.

Due to the similarity of the kinematic chains in the mechanism, only one of them is shown with the index "*i*". As can be seen in Fig. 3, the origin of the global coordinate system is {O} and the components of this coordinate system are defined by x_o, y_o, and z_o. The vector connecting the origin of the global coordinate system and the starting rail of the prismatic joint is represented by $\boldsymbol{a_i}$. The local starting point of the rail is indicated by the vector $\boldsymbol{d_i}$, connecting it to the prismatic joint *i* on the carriage. The magnitude of the vector $\boldsymbol{l_i}$ seen in the figure is equal to the length of the connecting rod, *i*. Also, $\boldsymbol{c_i}$ is a vector starting from the midpoint of the spherical joints and ending in the rotary axis of the connector. However, for $i = 2, 4$, due to the nature of the mechanism, the vector $\boldsymbol{c_i}$ must be equal to 0. The vector $\boldsymbol{b_i}$ defined in Fig. 3 is defined as a vector fixed to the centre {P} of the moving platform, expressing the final position of the parallelograms with respect to the local frame. All kinematic relations are defined according to the fixed platform-dependent global framework {O}.

Considering Fig. 3, the vector equation for the *i*, the kinematic chain can be expressed as in (1)

$$\boldsymbol{p} + {}^{o}_{P}\boldsymbol{R}\,{}^{P}_{i}\boldsymbol{b} = {}^{o}_{i}\boldsymbol{a} + {}^{o}_{i}\boldsymbol{d} + {}^{o}_{i}\boldsymbol{l} + {}^{o}_{i}\boldsymbol{c}. \quad (1)$$

In this equation, the transformation expression given below should be used to define the vector $\boldsymbol{b_i}$ according to the global coordinate system

$$ {}^{o}_{i}\boldsymbol{b} = {}^{o}_{P}\boldsymbol{R}\,{}^{P}_{i}\boldsymbol{b}. \tag{2} $$

The ${}^{o}_{P}\boldsymbol{R}$ expression in (2) is the rotation matrix, and it is defined only in the ***x***-direction, as expressed in (3), due to the mechanical structure of the system. In other words, the rotation matrix $R_X(\theta)$ expressed in (3) is included in (2) due to the ability of the system to rotate around the x-axis due to its four motors. The rotational motion of the moving table around the z-axis is made by an independent 5th motor placed under the table. Therefore, the rotation matrix $R_z(\theta)$ is not included in the kinematic equation

$$ {}^{o}_{P}\boldsymbol{R} = \boldsymbol{R}_X(\boldsymbol{\theta}) = \begin{bmatrix} 1 & 0 & 0 \\ 0 & \cos(\theta)_x & -\sin(\theta)_x \\ 0 & \sin(\theta)_x & \cos(\theta)_x \end{bmatrix}. \tag{3} $$

The vectors ${}^{o}_{i}\boldsymbol{d}$ and ${}^{o}_{i}\boldsymbol{c}$ in (1) are always parallel to each other. Therefore, since $\hat{\boldsymbol{d}}_t$ is the unit vector of $\boldsymbol{d_i}$, (1) can be rewritten as in (4)

$$ (\boldsymbol{p} + \boldsymbol{b_i} - \boldsymbol{a_i} - c_i\hat{\boldsymbol{d}}_t) \; - \; \boldsymbol{L_i} \; = \; d_i\hat{\boldsymbol{d}}_t \,. \tag{4} $$

Here, c_i and d_i represent the magnitudes of the vectors $\boldsymbol{c_i}$ and $\boldsymbol{d_i}$, respectively. The vector $\boldsymbol{L_i}$ is denoted by l_i, and its value is unknown. In this case, the left side of the equation given above represents a sphere with centre $\boldsymbol{p} + \boldsymbol{b_i} - \boldsymbol{a_i} - \boldsymbol{c_i}\hat{\boldsymbol{d}}_t$ and radius l_i, and the right side of (4) represents a line passing through the origin and through $\boldsymbol{d_i}$. Therefore, solving (4) is equivalent to getting the intersection of a known sphere and a line in space. Using the equivalences mentioned above, d_i can be obtained as follows

$$ \boldsymbol{d_i} = -\boldsymbol{c_i} + \hat{\boldsymbol{d}}_i^T(\boldsymbol{p} + \boldsymbol{b_i} - \boldsymbol{a_i}) \pm $$
$$ \pm\sqrt{\boldsymbol{l}_i^2 - (\boldsymbol{p} + \boldsymbol{b_i} - \boldsymbol{a_i})^T(\boldsymbol{I}_{3\times3} - \hat{\boldsymbol{d}}_t\hat{\boldsymbol{d}}_i^T)(\boldsymbol{p} + \boldsymbol{b_i} - \boldsymbol{a_i})}. \tag{5} $$

When the position and orientation values of the mechanism are defined with the help of (5) obtained by vector analysis, the length d_i that will bring the mechanism to these positions and orientation values can be calculated.

B. Workspace of the Recommended 5-DOF 3D Printer

As is known, it is very easy to determine the workspace of general machine tools with three vertical axes (x, y, z) connected in series. However, if the number of axes is increased, some restrictions arise, and these restrictions cause some problems in determining the working space. Similarly, some difficulties are encountered in determining the working space due to the lack of a fixed orthogonal axis in machine tools with a parallel structure. The working space of the parallel mechanism is obtained by considering the kinematic parameters or constraints of the structure. For this reason, the workspace that will be created by considering all the constraints does not have a regular geometric shape. Due to this irregular geometric shape, the use of parallel mechanisms is a disadvantage in terms of workspace. To minimize this disadvantage, it is necessary to determine the best operating range for the system. In the literature, optimization methods have been used in study workspace analyses for different types of parallel mechanisms taking into account the limitations of the mechanism.

Within the scope of this study, an optimization algorithm was developed to obtain the working space of the designed parallel mechanism taking into account the constraints. The algorithm developed in this method scans the entire working area of the machine according to the position of the point in the working area and then verifies each point in the working space by checking the physical constraints or the limit of parallel machine tools. In general, the workspace analysis algorithm can be divided into three main stages:

– Search algorithm to find the working space range;
– Transforming inverse kinematics;
– Testing physical constraints or machine limit.

In the algorithm, transforming the inverse kinematics after providing the moving platform position (position and orientation) from the search algorithm provides the basic position for testing the physical limitations of the machine. Scanning processes are started by dividing the workspace into x - y planes or z spaces into fixed horizontal sections; then scanning of the next plane is started after all points of the plane are scanned.

If the movement range of the car on the rail is within the allowable range, the points considered will be within the working space. This limit is expressed as in (6)

$$ \boldsymbol{d}_{\min} \le \boldsymbol{d}_i \le \boldsymbol{d}_{\max}. \tag{6} $$

In the designed mechanism, attention should be paid to the angle that is likely to collide between the rail and the moving platform, and this is shown in Fig. 4. The necessary condition to prevent the collision of the moving platform and the rail is expressed in (7)

$$ \boldsymbol{\theta}_{critical} \le \boldsymbol{\gamma}. \tag{7} $$

Fig. 4. Angle constraint between the moving platform and the rail.

The next angle to consider is θ_j. This angle represents the maximum lateral angle that the legs attached to the movable platform can make with the fixed rail, as shown in Fig. 5. The maximum allowable value for this angle is 30 degrees. On the other saying,

$$\boldsymbol{\theta}_j \leq \frac{\boldsymbol{\pi}}{\mathbf{6}}. \tag{8}$$

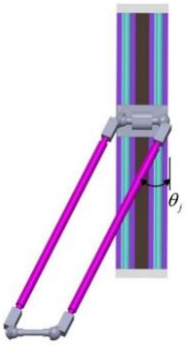

Fig. 5. Limitation of the maximum allowable lateral angle.

In the proposed mechanism, there is a possibility of collision with the platform to which the leg tip connected to the moving platform is attached, as shown in Fig. 6. For this reason, this angle should be chosen with a small value when optimizing the working space.

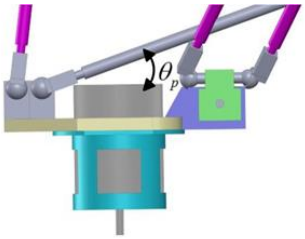

Fig. 6. Mobile platform restriction.

In this study, a workspace optimization algorithm is implemented in Matlab offline taking into account all the limitations mentioned above. In the Matlab offline algorithm developed, first, the angle constraint between movable platform and rail situation expressed in Fig. 4 has been taken into account, and then the algorithm has been run according to the limitation of the maximum allowable lateral angle restriction expressed in Fig. 5. Finally, according to the mobile platform restriction expressed in Fig. 5, the appropriate workspace has been obtained. The workspace of the designed system is shown in Fig. 7.

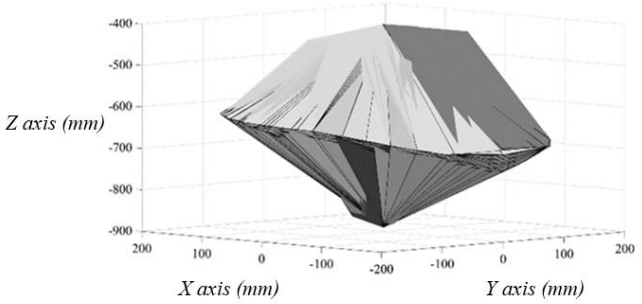

Fig. 7. Workspace of the designed system.

C. Velocity Kinematic Analysis of a 5-DoF 3D Printer

To define the velocity vector $\dot{\boldsymbol{p}}$ of the moving platform of the mechanism, the derivative of (4) must be taken in terms of time

$$\dot{\boldsymbol{p}} + \dot{\theta}\hat{\boldsymbol{i}} \times \boldsymbol{b}_i = \dot{d}_i \hat{\boldsymbol{d}}_i + \boldsymbol{\omega}_{li} \times \boldsymbol{I}_i. \tag{9}$$

In this equation, $\dot{\theta}$ is the angular velocity amplitude of the moving platform. In the case of scalar multiplication with the vector $\boldsymbol{I_i}$ of both sides of (9), (10) is obtained

$$\dot{d}_i = \frac{\boldsymbol{I}_i}{\hat{\boldsymbol{d}}_i \boldsymbol{I}_i}.\boldsymbol{p} + \frac{(\hat{\boldsymbol{i}} \times \boldsymbol{b}_i).I_i}{\hat{\boldsymbol{d}}_i.\boldsymbol{I}_i}.\dot{\theta}. \tag{10}$$

Thus, using (10), the matrix representation of the velocity kinematics that transforms the moving platform from an angular form to a linear form is obtained as in (11)

$$\begin{bmatrix} \dot{d}_1 \\ \vdots \\ d_4 \end{bmatrix} = \begin{bmatrix} \frac{\boldsymbol{I}_1^T}{\hat{\boldsymbol{d}}_1.\boldsymbol{I}_1} & \frac{(\boldsymbol{b}_1 \times \boldsymbol{I}_1).\hat{\boldsymbol{i}}}{\hat{\boldsymbol{d}}_1.\boldsymbol{I}_1} \\ \vdots & \vdots \\ \frac{\boldsymbol{I}_4^T}{\hat{\boldsymbol{d}}_4.\boldsymbol{I}_4} & \frac{(\boldsymbol{b}_4 \times \boldsymbol{I}_4).\hat{\boldsymbol{i}}}{\hat{\boldsymbol{d}}_4.\boldsymbol{I}_4} \end{bmatrix} \begin{bmatrix} \dot{\boldsymbol{p}} \\ \dot{\theta} \end{bmatrix} = \boldsymbol{J} \begin{bmatrix} \dot{\boldsymbol{p}} \\ \dot{\theta} \end{bmatrix}. \tag{11}$$

$\boldsymbol{J}$, expressed in (11), represents the Jacobian matrix of the system.

IV. Design of Electrical Sub-Components of a 5-DOF 3D Printer

As expressed in the mechanical structure of the designed 3D printer, 5-step motors are used in the system. 4 motors placed at the bottom of the system provide 3 translational and 1 rotational motion to the moving table with kinematic analysis. The other motor located in the lower part of the movable table provides the rotation of the movable table on the z-axis. To precisely manufacture a part designed in 3D space, the motors must be accurately controlled based on inverse kinematic analysis. The complete block diagram of the instrumentation/electronic system is shown in Fig. 8. As shown in Fig. 8, the flow chart has been started with the generation of a 3D solid CAD model. Then the model has been converted into the standard STereoLithography (STL) file format and generated into G-Code. These codes have been converted into reference trajectories that motors have to follow using kinematic analysis interface software. These reference trajectories then have been fed in as the set points for the four local controllers. The controller then has applied the necessary control action to the hybrid stepper motor drivers, which in turn allows the correct rotations.

In this study, a 4-layer precision control board is designed using TMC262 stepper motor drivers that can work with the STM32F405RB microprocessor as shown in Fig. 9. The TMC262 is specially designed to drive 2-phase stepper motors with high-resolution sinusoidal microstepping. In addition, it can measure sensorless mechanical load and drive a step motor with adaptive power optimization and low-resonance chopper control. In addition, the TMC429 integrated circuit is used to create a motion profile for the stepper motor. According to the position, velocity, and acceleration information given by the TMC429 digital interface, it creates a trapezoidal motion profile and applies sequential step input to the TMC262 integrated circuit. The

main task of the STM32F405RB ARM Cortex M4 168 MHz processor shown in Fig. 9 is to run the equations obtained by kinematic analysis and send the appropriate codes to the TMC429.

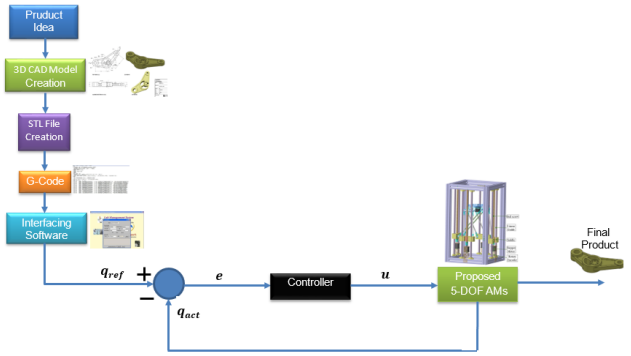

Fig. 8. Block diagram of the instrumentation/electronic system.

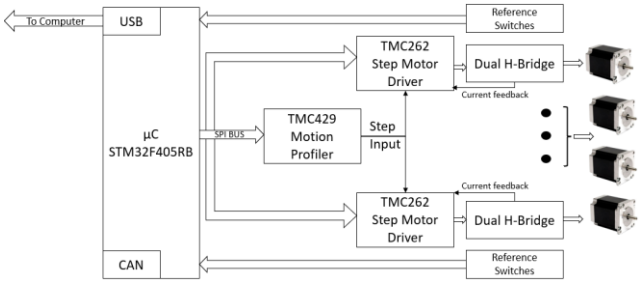

Fig. 9. Block diagram of the control board of the system [13].

In this study, first of all, the necessary components have been determined and the drawing of the printed circuit has been carried out to design the control structure shown in Fig. 10. The printed circuit board has been designed with 4 layers. Intermediate layers have been used for power and grounding. The power electronics elements and the digital electronics elements have been separated by the islanding method. The grounding islands have been connected by filtering, and in this way, the effect of the noise from the power elements on the digital electronic elements has been reduced. The supply input has been protected against short circuits and overvoltage with a transient-voltage-suppression (TVS) diode and SMT fuse. Printed circuit drawings are shown in the pictures in Fig. 10.

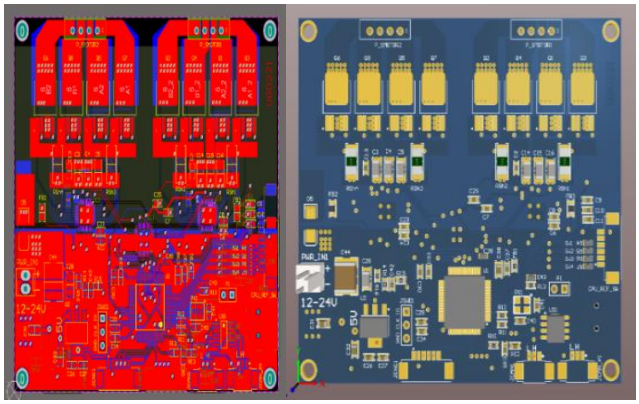

Fig. 10. Printed circuit drawings of the designed driver board.

To dissipate the heat generated in the MOSFET arrays, the broad slewing and vialing technique has been applied. Integrated drivers have been used to drive MOSFET arrays. Noise effects have been reduced by filtering communication lines and digital inputs. Electronic components have been selected as lead-free. The pads on the printed circuit board have been produced by the gold dipping method. In this way, the conductivity has increased and oxidation has been reduced. Component supply has been carried out following the completion of the printed circuit board production. Composition processes have been carried out using liquid solder and a printed circuit template (stencil). The strings of 4 driver cards have been made to be used in the system. The driver card, whose string has been completed, is shown in Fig. 11.

Fig. 11. Designed driver card.

The designed driver board can operate in the 12 V–24 V input voltage range and can transfer current up to 5 Amps to the motor coils. In addition to this, the current flowing through the motor coils can be measured with low tolerance shunt resistors. In this way, each stepper motor is driven by current feedback with a switching element containing 4 N-P MOSFET arrays. The driver has a current-controlled microstepping feature. The designed driver allows positioning up to 256 microsteps. In this way, one revolution of the stepper motor with 1.8 degree/step feature can be controlled with a resolution of 51200 steps. Thanks to this feature, the driver is capable of high torque and precise positioning. In addition to all these features, the driver has a Controller Area Network (CAN). Commands in G-Code format received from the computer are transmitted to the relevant motors over this CAN network.

In this study, an interface software has been developed in the open-source Qt development environment to transfer the G-CODE files of the CAM/CAD model to the designed driver card. The interface of the software is presented in Fig. 12.

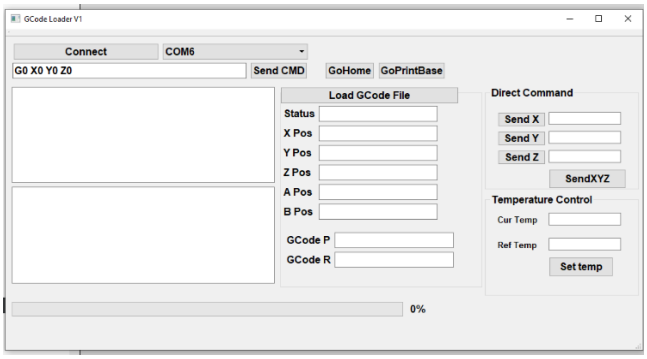

Fig. 12. The interface program of the designed driver card.

V. DESIGN OF 5-DOF 3D PRINTER SYSTEM

After modelling and mathematical analysis of the parallel

mechanism, the construction phase of all components was started. Considering the inverse kinematics and workspace of the modelled system, the mechanical sub-components of the system were designed, and all the designed sub-components were assembled and calibrated. The pictures of the designed mechanical sub-components and the calibration procedures for these components are presented in Fig. 13. For the calibration process, millimetric measurements were made using callipers since each leg should be the same length. However, a comparator was used to determine whether the legs were straight. For the moving platform to remain level, the locations of the start switches located at the bottom of the mechanism were determined by millimetric measurement using a calliper.

The foot graph of the system, whose design was completed by bringing together all system components, is presented in Fig. 14.

Fig. 13. Mechanical sub-components and calibration processes.

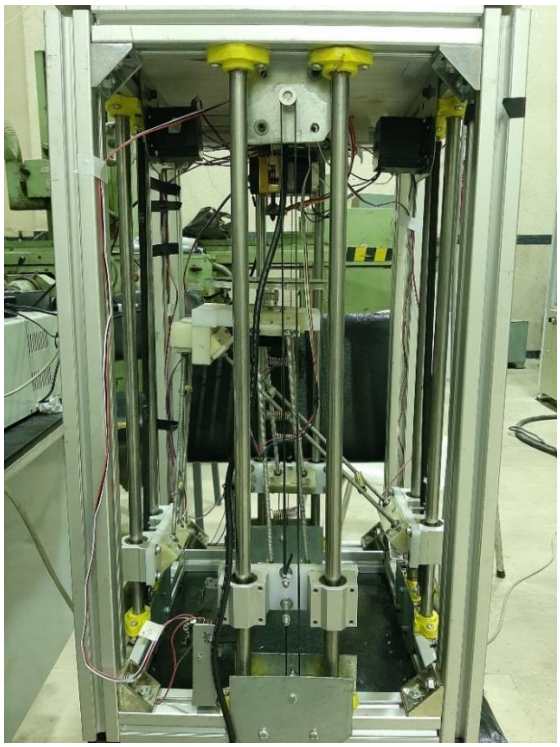

Fig. 14. Designed 5-DOF Parallel 3D Printer.

VI. EXPERIMENTAL APPLICATION

After all, the mathematical analyses of the designed system have been done, and the test studies of the system have been started. To automatically produce complex protruding components, an efficient versatile slicing algorithm is required to divide CAD models into a series of suitable layers. A new method concept for multidirectional slicing of CAD models is represented in STL format. The input of the control program is a standard STL file most commonly used to represent CAD models in the rapid prototyping process planning. In an ASCII STL file, the model is represented using triangular directions. Figure 15 shows an example of the STL format and its 3D model.

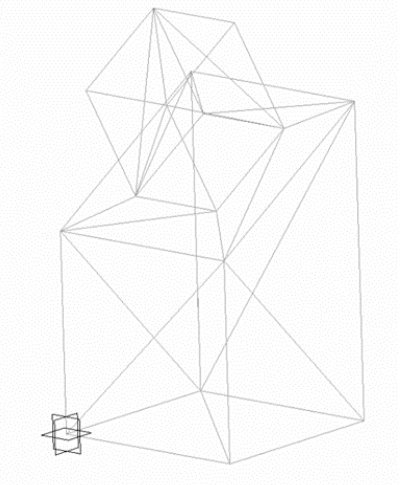

Fig. 15. A sample of the STL format and its 3D model.

An input primary STL model (Fig. 15) is first decomposed using a simple curvature-based segmentation method. Accordingly, each sub-part can be built in one direction. Next, the sub-species are sequentially sliced separately along the appropriate associated product directions.

The parsing algorithm for generating multi-directional slices includes two modules: part parsing and structure direction identification. The part separation module first decomposes a complex part into several sub-parts using the curvature-based separation method gradually. A depth tree structure is then created based on topology information to regroup the sub-units and provide the sequence of sequences for the next slicing module. The primary part shown in Fig. 16 is decomposed into two sub-parts by a stepwise separation process. With the versatile deposition algorithm used in this article, the part can be produced without support. The CAM unit also uses a hole-filling algorithm to close the open faces of the sub-parts. The filling face of the sample piece is shown in Fig. 17. The input to this algorithm is the simplified STL model with all the blanks filled.

Then, according to the order of each sub-part, the slices of each sub-part along its optimal build direction can be generated simultaneously. The translator unit is one of the most important parts of a 3D printer. The interpreter converts the codes produced by the CAM units into the moving information of the 3D printer robot. In this study, a special CAM interpreter was used according to the robot mechanism. An example of useful G-Codes according to the parallel robot mechanism is shown in Fig. 18.

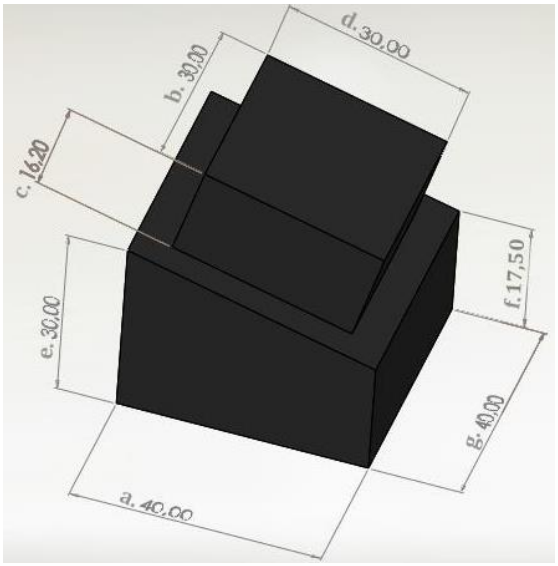

Fig. 16. A complicated primary model.

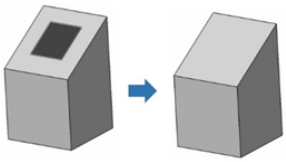

Fig. 17. Covering the whole of one face.

```
G01 X0.0 Y10.0 Z0.01 E280.0
G00 X5.0 Y-10.0 Z0.01
G01 X5.0 Y10.0 Z0.01 E300.0
G00 X-10.0 Y-5.0 Z0.01
G01 X10.0 Y-5.0 Z0.01 E320.0
G00 X-10.0 Y0.0 Z0.01
G01 X10.0 Y0.0 Z0.01 E340.0
G00 X-10.0 Y5.0 Z0.01
G01 X10.0 Y5.0 Z0.01 E360.0
G00 X10.0 Y10.0 Z0.51
G01 X-9.32 Y10.0 Z0.51 E379.32
G01 X-10.0 Y10.0 Z0.51 E380.0
G01 X-10.0 Y8.679 Z0.51 E381.321
```

Fig. 18. G-Code generation using a CAM unit.

The methods presented in this research have been implemented by programs written in Python and C++. In this paper, as a case study introduced in Fig. 16, a complex part is decomposed into two parts as shown in Fig. 17, and then the hole of the upper face of the lower part is closed using the proposed algorithm. Then, each of the parts was sliced and tool paths were created using the proposed slicing algorithm. Finally, the G-Codes created in the translator unit were created and sent to the control unit. The designed part was produced without the need for any support. This part is shown in Fig. 19. As seen in the figure, the produced part is compatible with Fig. 16 and it has been proven that the system kinematics works correctly. The size comparison between the sample piece shown in Fig. 16 and the manufactured piece shown in Fig. 19 is presented in Table I.

TABLE I. COMPARISON TABLE FOR ALL DIMENSIONS.

Name of the side length	Original part (mm)	Produced part (mm)	Difference between parts (mm)
a	40	38,5	1,5
b	30	29,5	0,5
c	16,2	17	0,8
d	30	30,5	0,5
e	30	28,5	1.5
f	17,5	16,5	1.0
g	40	38,5	1,5

As can be seen in Table I, there are small differences between the two parts. The main reason for the small differences is that the designed system is a prototype system and is not commercial. Moreover, a video link of our presented work will be given as follows: https://youtu.be/vbuJpNbITlc

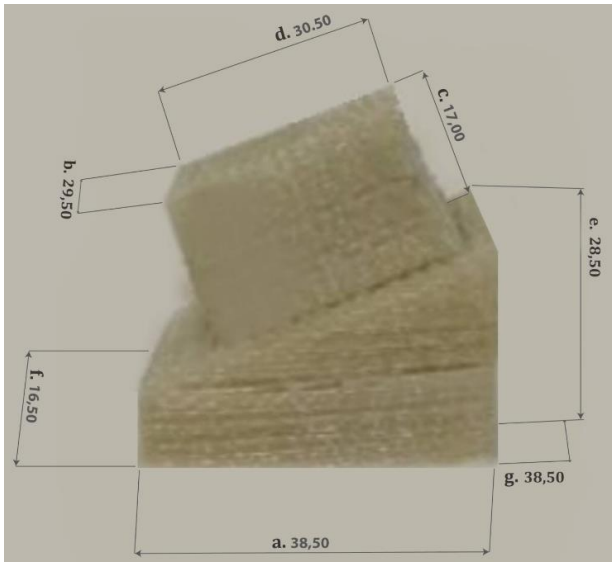

Fig. 19. A sample part produced by a 5-DOF parallel robot.

VII. CONCLUSIONS

In this study, information on the mathematical analysis and design of a new 5-DOF 3D printer that can be used in additive manufacturing technologies is presented. The inverse kinematic equations of position and velocity have been obtained based on the concept of a closed-loop vector chain. Afterwards, the workspace of the mechanism has been derived by taking into account all the constraints of the system. The most important feature of the developed system compared to other systems on the market is that it has more degrees of freedom. Due to the added rotational movement of the x-axis and z-axis, it is aimed to increase the speed of machining and minimize the number of support parts that may be needed during production. According to the experimental results, it was observed that the designed 3D printer made a maximum error of 1.5 mm in the production of a sample part. In addition, the production time of the sample piece was approximately 18 minutes. This time is considered to be a reasonable time compared to conventional 3-DOF printers. It is obvious that if the system designed as a prototype is calibrated better and servo motors are used instead of step motors, the system will operate with better precision. However, non-linear control methods will be used for system position controls in future studies. Thus, the sensitivity of the system will increase even more.

CONFLICTS OF INTEREST

The authors declare that they have no conflicts of interest.

REFERENCES

[1] L. Li, A. Haghighi, and Y. Yang, "A novel 6-axis hybrid additive-subtractive manufacturing process: Design and case studies", *Journal of Manufacturing Processes*, vol. 33, pp. 150–160, Jun. 2018. DOI: 10.1016/j.jmapro.2018.05.008.

[2] A. Kampker, J. Triebs, S. Kawollek, P. Ayvaz, and S. Hohenstein,

"Review on machine designs of material extrusion based Additive Manufacturing (AM) systems - Status-quo and potential analysis for future AM systems", *Procedia CIRP*, vol. 81, pp. 815–819, 2019. DOI: 10.1016/j.procir.2019.03.205.

[3] P. Urhal, A. Weightman, C. Diver, and P. Bartolo, "Robot-assisted additive manufacturing: A review", *Robotics and Computer-Integrated Manufacturing*, vol. 59, pp. 335–345, Oct. 2019. DOI: 10.1016/j.rcim.2019.05.005.

[4] L. Wang, J. Wu, J. Wang, and Z. You, "An experimental study of a redundantly actuated parallel manipulator for a 5-DOF hybrid machine tool", *IEEE/ASME Transactions on Mechatronics*, vol. 14, no. 1, pp. 72–81, 2009. DOI: 10.1109/TMECH.2008.2008096.

[5] R. Clavel, "Unmanned robotic delta weapon platform", WIPO patent, WO 87/03528, 1987.

[6] F. Xie and X.-J. Liu, "Analysis of the kinematic characteristics of a high-speed parallel robot with Schönflies motion: Mobility, kinematics and singularity", *Frontiers of Mechanical Engineering*, vol. 11, pp. 135–143, 2016. DOI: 10.1007/s11465-016-0389-7.

[7] F. Pierrot and O. Company, "H4: A new family of 4-DOF parallel robots", in *Proc. of 1999 IEEE/ASME International Conference on Advanced Intelligent Mechatronics (Cat. No.99TH8399)*, 1999, pp. 508–513. DOI: 10.1109/AIM.1999.803222.

[8] O. Company, S. Krut, and F. Pierrot, "Modelling of a 4 axis parallel machine for heavy parts handling", *Proceedings of the Institution of Mechanical Engineers, Part K: Journal of Multi-body Dynamics*, vol. 216, pp. 1–12.

[9] E. Fiore, H. Giberti, and L. Sbaglia, "Dimensional synthesis of a 5-DOF parallel kinematic manipulator for a 3d printer", in *Proc. of 2015 16th International Conference on Research and Education in Mechatronics (REM)*, 2015, pp. 41–48. DOI: 10.1109/REM.2015.7380372.

[10] A. J. Alvares, E. A. R. Gasca, and C. I. R. Jaimes, "Development of the linear Delta robot for additive manufacturing", in *Proc. of 2018 5th International Conference on Control, Decision and Information Technologies (CoDIT)*, 2018, pp. 187–192. DOI: 10.1109/CoDIT.2018.8394869.

[11] R. Celi, A. Sempértegui, D. Morocho, D. Loza, D. Alulema, and M. Proaño, "Study, design and construction of a 3D printer implemented through a delta robot", in *Proc. of 2015 CHILEAN Conference on Electrical, Electronics Engineering, Information and Communication Technologies (CHILECON)*, 2015, pp. 717–722. DOI: 10.1109/Chilecon.2015.7404650.

[12] M. Mahboubkhah and A. Barari, "Design and development of a novel 4-DOF parallel kinematic coordinate measuring machine (CMM)", *International Journal of Computer Integrated Manufacturing*, vol. 32, no. 8, pp. 750–760, 2019. DOI: 10.1080/0951192X.2019.1610576.

[13] *TMC Data Manual*, TRINAMIC Motion Control Inc. [Online]. Available: https://www.trinamic.com/fileadmin/assets/Products/ICs_Documents/TMC262_TMC262C_datasheet_Rev2.25.pdf